International Journal of Heat and Mass Transfer 126 (2018) 479–488

Contents lists available at ScienceDirect

International Journal of Heat and Mass Transfer

journal homepage: www.elsevier.com/locate/ijhmt

The effect of conducting bounding horizontal plates on species separation in porous cavity saturated by a binary mixture

Abdelkader Mojtabi [a,b,*], Bafétigué Ouattara [a,b,d], D. Andrew S. Rees [c], Marie-Catherine Charrier-Mojtabi [a,b]

[a] Université de Toulouse, INPT, UPS, IMFT (Institut de Mécanique des Fluides deToulouse), Allée Camille Soula, F-31400 Toulouse, France
[b] CNRS, IMFT, F-31400 Toulouse, France
[c] Department of Mechanical Engineering, University of Bath, Bath BA2 7AY, UK
[d] Université Nangui Abrogoua, UFR Sciences Fondamentales Appliquées, 02 BP 801 Abidjan 02, Cote d'Ivoire

ARTICLE INFO

Article history:
Received 21 February 2018
Received in revised form 7 May 2018
Accepted 9 May 2018

Keywords:
Convection
Soret effect
Thermogravitational-diffusion
Stability
Species separation
Porous medium

ABSTRACT

In this paper, an analytical and numerical study of species separation in binary mixtures taking account of the presence of bounding plates for the cell is presented. A rectangular horizontal porous cavity saturated by a binary mixture and heated from below is considered. This cavity is bounded by thin plates of uniform thickness, the outer surfaces of which are subjected to a constant heat flux. The transition from the equilibrium solution to the convective one, either stationary or oscillatory, was previously studied by Ouattara et al. (2012). Thus in the first part of this paper, the critical parameters associated with the onset of long wavelength disturbances, obtained analytically, are recalled. Then the hypothesis of parallel flow is used to determine an analytical solution which describes the unicellular flow which may appear in the case of a large aspect ratio cell for a given range of separation ratio, ψ, Rayleigh number, *Ra*, Lewis number, Le, the ratio of the plate to the porous layer thickness, δ, and their thermal conductivity ratio, *d*. The analytical results are corroborated by direct numerical simulations. We verify that if *d* goes to infinity, the walls become infinitely conductive and we find the results obtained by Charrier-Mojtabi et al. (2007). When *d* tends to 0, the walls become infinitely thin the results obtained by Yacine et al. (2016) are recovered.

A linear stability analysis of the unicellular flow is also presented. The eigenvalue problem resulting from the temporal stability analysis is solved by a Tau spectral method. The optimal Rayleigh number leading to an optimal value of the separation horizontal gradient is determined for different values of physical parameters. We show that the species separation depends sensitively on the ratio of the plate to the porous layer thickness, and the ratio of their thermal conductivities. Furthermore, we have shown that in the stationary state and for a given value of the thermal conductivity ratio ($d = 29$), the maximum separation is almost equal for walls of the same thickness than the one of porous cavity or for the case of porous cell delimited by the infinitely thin walls.

1. Introduction

In binary fluid mixtures subjected to temperature gradient, a mass fraction gradient appears due to the thermodiffusion or Soret effect. In addition to the usual expression for the mass flux $\vec{J}$ given by Fick's law, a part due to the temperature gradient is added so that:

$$\vec{J} = -\rho D \nabla C' - \rho D'_T \nabla T'$$

where D is the mass diffusion coefficient, ρ the density, and C' the mass fraction of the denser component. Here $D'_T = F(C')D_T$, where D_T is the thermodiffusion coefficient and $F(C')$ is a particular function of C' satisfying both $F(C'=0)=0$ and $F(C'=1)=0$. Most authors use the function, $F(C') = C'(1-C')$ and make the assumption that $C'(1-C') \approx C_0(1-C_0)$ where C_0 is the initial value of the mass fraction.

Under the gravity field, the coupling between convection and thermo-diffusion, called thermo-gravitational diffusion, has been found to lead to species separation. Thermo-gravitational separation in a porous medium which is saturated by a binary mixture has been studied widely because of its numerous fundamental and industrial applications. Some examples of interest are the migration of moisture in fibrous insulation, the transport of

* Corresponding author at: Université de Toulouse, INPT, UPS, IMFT (Institut de Mécanique des Fluides deToulouse), Allée Camille Soula, F-31400 Toulouse, France.
E-mail address: mojtabi@imft.fr (A. Mojtabi).

https://doi.org/10.1016/j.ijheatmasstransfer.2018.05.046
0017-9310/

Nomenclature

A	aspect ratio of the porous bulk $A = L/H$
a	effective thermal diffusivity of the porous-mixture system $a = \lambda_p/(\rho c)_f$
a_s	thermal diffusivity of metal $a_s = \lambda_s/(\rho c)_s$
C	mass fraction of denser component of the mixture
C_0	initial mass fraction of the denser component of the mixture
m	mass fraction gradient along the horizontal axis
m^r	real mass fraction gradient along the horizontal axis
d	thermal conductivity ratio $d = \lambda_s/\lambda_p$
D^*	mass diffusion coefficient ($m^2\ s^{-1}$)
D_T^*	thermodiffusion coefficient ($m^2\ s^{-1}\ K^{-1}$)
H	height of the porous layer (m)
h	height of the horizontal plates (m)
K	permeability of the porous medium (m^2)
k	wave number
k_c	critical wave number
L	length of the cavity (m)
Le	Lewis number $Le = a/D^*$
q'	uniform heat per unit area ($W{\cdot}m^{-2}$)
Ra	Darcy-Rayleigh number $Ra = (KHg\beta_T\Delta T)/(av)$
Ra_c	critical Rayleigh number
t	nondimensional time (s)
T_1, T_3	temperatures inside the lower and upper plates (K)
T_2	temperature inside the porous bulk (K)
$\vec{\mathbf{V}}$	flow velocity (ms^{-1})
u, v	Horizontal and vertical velocity components (ms^{-1}

Greek symbols

β_T	thermal expansion coefficient (K^{-1})
β_C	solutal expansion coefficient
ε^*	porosity of porous medium
ε	normalized porosity of the porous medium
δ	ratio of the plate to the porous layer thickness $\delta = h/H$
ρ	density of the mixture ($kg\ m^{-3}$)
ψ	separation ratio $\psi = -(\beta_C/\beta_T)(D_T^*/D^*)C_0(1-C_0)$
ψ_{uni}	separation ratio beyond which flow at onset of convection is unicellular
λ_p	effective thermal conductivity of the saturated porous medium ($W\ m^{-1}\ K^{-1}$)
λ_s	thermal conductivity of the horizontal plates ($W\ m^{-1}\ K^{-1}$)
$(\rho c)_f$	volumetric heat capacity of the mixture ($J\ m^{-3}\ K^{-1}$)
$(\rho c)_p$	effective volumetric heat capacity of saturated porous medium ($J\ m^{-3}\ K^{-1}$)
v	kinematic viscosity of mixture ($m^2\ s^{-1}$)
φ	stream function
θ_1, θ_3	temperature perturbations inside the lower and upper plates
θ_2	bulk temperature perturbation
α	thermal diffusivity ratio $\alpha = a_s/a$

Superscripts

$'$	dimensional variable

contaminants in saturated soil, drying processes or solute transfer in the mushy layer during the solidification of binary alloys.

Reviews of recent developments and publications in this field are given by Nield and Bejan [1], Ingham and Pop [2], Vafai [3] and more recently by Vadasz [4]. A compilation of the most pertinent information on the critical Rayleigh number and wavenumber associated to the onset of convection in an infinite porous layer saturated by a mono-constituent fluid with different boundary conditions, (i.e. free or impermeable; prescribed temperature or prescribed heat flux) may be found in Nield and Bejan [1].

Zebib and Bou-Ali [5] performed a linear stability analysis of a binary mixture buoyant return flow in a tilted, differentially heated, infinite layer using an asymptotic long-wave analysis and pseudo-spectral Chebyshev numerical solutions. For negative separation ratio, it was shown that longitudinal instabilities with small wave numbers are triggered at any finite temperature difference for all inclination angles except when the layer is close to the horizontal for either the heating-from-above or heating-from-below configurations. Numerical results were given for a specific water-ethanol mixture and were in good agreement with the asymptotic results. Transition from the longitudinal stationary instabilities in inclined layers to these instabilities in horizontal layers was also presented for this mixture.

With regard to thermo-gravitational separation, in 1938, Clusius and Dickel [6] successfully carried out the separation of gas mixtures in a vertical cavity heated from the side (thermo-gravitational column, TGC). Furry et al. [7] then developed the theory of thermodiffusion to explain the experimental process involved in isotope separation. For differentially-heated vertical columns, the authors showed that there is a maximum separation for an optimal value of the cell thickness. Subsequently, many works have followed, in order to justify the assumptions or extending the results of the FJO theory to the case of binary liquids. Lorenz and Emery [8] proposed to introduce a porous medium into the cavity in order to increase the width of the cell corresponding to the maximum separation.

Bennacer et al. [9] studied the double diffusive convection in a vertical annular porous medium subjected to a horizontal temperature gradient. An increase in the curvature of the cylindrical annulus permits a higher species separation due to the nonsymmetrical temperature profile. To overcome such limitations, two sub-domains allowing filtration separation were proposed and investigated. The separation ability increases with the partitioning number. In the same configuration, and for double diffusive convection without Soret effect, Marcoux et al. [10] showed the curvature effect on the temperature and mass fraction field. More recently Abahri et al. [11], studied the separation of a binary mixture occurring in a horizontal porous annular layer. The inner and outer cylinders were kept at different and constant uniform temperatures Ti and To, with Ti < To. They used the perturbation method by developing the temperature, stream function and mass fraction in terms of a power series in the Rayleigh number, to provide solutions for low Rayleigh number flow regimes. Direct numerical simulations, using the finite element method, were performed to corroborate the results obtained analytically.

Charrier-Mojtabi et al. [12] and Elhajjar et al. [13] presented an analytical and numerical stability analysis of Soret-driven convection in a porous cavity saturated by a binary fluid. The porous cavity is bounded by horizontal surfaces of either infinite or finite extent and it was heated either from below or from above. These horizontal plates were maintained at different but constant temperatures. From the linear stability analysis, the authors found that the equilibrium solution loses its stability via a stationary bifurcation or a Hopf bifurcation depending on the separation ratio and the normalized porosity of the medium. The role of the porosity is important: when it decreases; the stability of the equilibrium solution is reinforced. In

the case of long-wave disturbances, for $\psi < 0$ and for ψ higher than a particular value called ψ_{uni}, they observed that the unicellular flow leads to species separation between the two ends of the cell. Then, they studied the stability of this unicellular flow. For a cell heated from below and for $\psi > \psi_{uni}$, the unicellular flow loses its stability via a Hopf bifurcation. Charrier-Mojtabi et al. [14] studied the species separation which appears at low Rayleigh number and for positive separation ratio in a porous horizontal slot submitted to a heat flux. The comparison with the separation obtained in differentially heated vertical columns (TGC) showed that even if the maximum value of the separation is the same in both configurations, the use of horizontal cells submitted to heat flux allowed height higher than the width of TGC column, increasing the amount of separated species significantly. More recently, Croccolo et al. [15] experimentally observed multiple convective structures in a circular cell filled with a binary mixture by varying very slightly the inclination of the experimental cell exhibiting strong confinement.

The main objective of this paper is to determine the effect of conducting bounding plates on the onset of a unicellular flow and to study its stability. Indeed the unicellular flow may lead to species separation only if this unicellular flow is stable. To our knowledge, there is no work on the species separation where the influence of the thickness and the nature of the bounding horizontal plates are taken into account even though the thickness of the plates in some applications may be greater than that of the fluid layer. Very few papers exist that consider the effect of the presence of horizontal bounding plates on the onset of thermal convection, the earliest being that of Riahi [16]. Later, Mojtabi and Rees [17] conducted a theoretical study of the effect of conducting bounding plates on the onset of Horton-Roger-Lapwood convection using both linear and nonlinear stability analyses. They showed that it is essential to determine the combined effect of the relative thickness of the bounding plates and the ratio of the conductivities of the plates and the saturated porous medium.

Rees and Mojtabi [18] considered the effect of conducting bounding plates on the onset of convection and the identity of the preferred weakly nonlinear post-critical convection planform. They presented regions in parameter space in which convection in the form of rolls is unstable and within which cells with square planform form the preferred pattern. Ouattara et al. [19] studied the effect of conducting boundaries on the onset of convection in a binary fluid-saturated porous layer. In this study, an analytical and numerical stability analysis was performed. The equilibrium solution is found to lose its stability via a stationary bifurcation or a Hopf bifurcation depending on the values of the dimensionless parameters. For the long wavelength mode, the critical Rayleigh number is obtained as $Ra_{cs} = 12(1 + 2d\delta)/[1 + \psi(2d\delta Le + Le + 1)]$ and $k_{cs} = 0$ for $\psi > \psi_{uni} > 0$.

In the present study we are mainly interested in the influence of the ratio of the bounding plates to the porous layer thickness and their conductivity ratio (See Fig. 1). In the first part, an analytical solution of the unicellular flow is developed in the case of a shallow cavity (aspect ratio $A >> 1$) and the amount of species separation (measured between the two horizontal ends of the cell) is expressed in terms of the thermal Rayleigh number, Lewis number, separation ratio, aspect ratio of the cell, the conductivity ratio and the thickness ratio of the bounding plates to the porous layer thickness. The value of the Rayleigh number leading to the maximum separation has been also obtained analytically. Then, in the second part, a linear stability analysis of the unicellular flow is presented using a Tau spectral method. The analytical results are corroborated by 2D direct nonlinear numerical simulations performed using a finite element method.

2. Mathematical formulation

We consider a rectangular cavity with large aspect ratio $A = L/H$, where L is the width in horizontal x' direction and H is the height of the cavity in the vertical y' direction (the gravity acceleration is $\vec{g} = -g\vec{y}$). The cavity is filled with a porous medium which is saturated by a binary fluid and the Soret effect is taken into account. This cavity is delimited above and below by two metal plates of uniform thickness, h. Neumann boundary conditions for temperature (i.e. a fixed uniform heat flux per unit area, q′) are applied on the outer horizontal surfaces of the composite layer at $y' = -h$ and at $y' = H + h$. The vertical walls ($x' = 0$, $x' = L$), are impermeable and insulated. All the boundaries are assumed to be rigid and impermeable. We also assume that Darcy's law is valid, and that the Oberbeck-Boussinesq approximation is applicable. The thermophysical properties of the binary fluid are considered constant except for the density in the buoyancy term, which varies linearly with the local temperature T' and the mass fraction C':

$$\rho = \rho_0[1 - \beta_T(T' - T_0) - \beta_C(C' - C_0)], \tag{1}$$

where β_T and β_C are the respective thermal and mass expansion coefficients of the binary fluid, and the temperature, T_0, and concentration, C_0, both correspond to the reference state. The value ρ_0 is the fluid mixture reference density at $T = T_0$ and $C = C_0$. Finally, T' is the dimensional temperature and C' the mass fraction of the denser component. We also use the other standard assumptions such as local thermal equilibrium between the phases and negligible viscous dissipation.

Thus the governing conservation equations for mass, momentum, energy and chemical species for the bulk are:

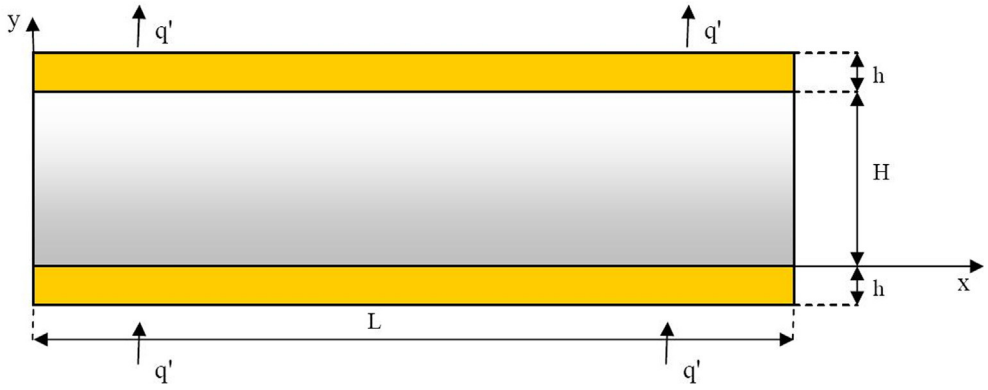

Fig. 1. Saturated porous medium of height H and length L bounded by two horizontal plates of thickness h. The upper and lower surfaces of the system are subject to a uniform heat flux. The vertical sidewalls are assumed to be perfectly insulated.

$$\begin{cases} \nabla^2\varphi' = -\frac{gK\beta_T}{\nu}\frac{\partial}{\partial x'}(T' + \frac{\beta_C}{\beta_T}C') \\ (\rho c)_p \frac{\partial T_2'}{\partial t'} + (\rho c)_f \vec{V}' \cdot \nabla T_2' = \lambda_p \nabla^2 T_2', \\ \varepsilon^* \frac{\partial C'}{\partial t'} + \vec{V}' \cdot \nabla C' = \nabla \cdot (D^* \nabla C' + C_0'(1 - C_0')D_T^* \nabla T_2'), \end{cases} \quad (2)$$

where V′ is the Darcy velocity, T_2' the temperature inside the porous bulk, ν the kinematic viscosity, $(\rho c)_p$ and $(\rho c)_f$ are the respective heat capacities of the saturated porous medium and the fluid, λ_p the effective thermal conductivity of the saturated porous medium, ε* its porosity, and φ' is the stream function. As usual the equation of continuity is satisfied by introducing the stream function according to: $u' = \partial\varphi'/\partial y'$ and $v' = -\partial\varphi'/\partial x'$.

In the two plates bounding the porous medium, the conduction heat transfer equation are:

$$\begin{aligned} (\rho c)_s \frac{\partial T_1'}{\partial t'} &= \lambda_s \nabla^2 T_1', \\ (\rho c)_s \frac{\partial T_3'}{\partial t'} &= \lambda_s \nabla^2 T_3', \end{aligned} \quad (3)$$

where T_1' and T_3' are the temperature inside the lower and upper plates, respectively, and $(\rho c)_s$ and λ_s are the heat capacity and the thermal conductivity of the solid plates. We assume that the bounding plates are made from the same material and are of equal thickness. The reference scales are H for the length, a/H for the velocity with $a = \lambda_p/(\rho c)_f$ (a is the effective thermal diffusivity of the porous mixture system), $H^2/(\lambda_p/(\rho c)_p)$ for the time ($(\rho c)_p$ is the effective volumetric heat capacity of saturated porous medium), $\Delta T = q'H/\lambda_p$ for the temperature, $\Delta C = -\Delta T C_0(1 - C_0)(D_T^*/D^*)$ for the mass fraction, where D_T^* and D^* are, respectively, the thermodiffusion and mass-diffusion coefficient of the denser component.

The dimensionless mathematical formulation of the problem is given by:

$$\begin{cases} \nabla^2\varphi = -Ra\frac{\partial}{\partial x}(T_2 + \psi C), \\ \frac{\partial T_2}{\partial t} + \vec{V} \cdot \nabla T_2 = \nabla^2 T_2, \\ \varepsilon \frac{\partial C}{\partial t} + \vec{V} \cdot \nabla C = \frac{1}{Le}(\nabla^2 C - \nabla^2 T_2), \\ \frac{\partial T_1}{\partial t} = \alpha \nabla^2 T_1, \\ \frac{\partial T_3}{\partial t} = \alpha \nabla^2 T_3. \end{cases} \quad (4)$$

The problem under consideration depends on eight non-dimensional parameters: the thermal Rayleigh number, $Ra = (g\beta_T K \Delta T H)/(a\nu)$ (K is the permeability of the porous medium); the separation ratio $\psi = -(\beta_C/\beta_T)(D_T^*/D^*)C_0(1 - C_0)$; the Lewis number $Le = a/D^*$; the normalized porosity, $\varepsilon = \varepsilon^*(\rho c)_f/(\rho c)_p$; the thermal diffusivity ratio, $\alpha = a_s/a_p$ where $a_s = \lambda_s/(\rho c)_s$ and $a_p = \lambda_p/(\rho c)_p$ are respectively the thermal diffusivity of the solid bounding plates and the porous medium; the thermal conductivity ratio, $d = \lambda_s/\lambda_p$; the ratio of the plate to the porous layer thickness $\delta = h/H$, and the aspect ratio of the cell $A = L/H$.

In the present study, the intensity of the thermal buoyancy forces is expressed only in terms of the thermal Rayleigh number, Ra.

The corresponding dimensionless boundary and interface conditions are:

$$\begin{aligned} &for \quad y = -\delta, && \frac{\partial T_1}{\partial y} = -\frac{\lambda_p}{\lambda_s} = \frac{-1}{d}; \\ &for \quad y = 0, && \frac{\partial T_1}{\partial y} = \frac{1}{d}\frac{\partial T_2}{\partial y}, \quad T_1 = T_2, \quad \varphi = 0, \quad \frac{\partial C}{\partial y} - \frac{\partial T_2}{\partial y} = 0; \\ &for \quad y = 1, && \frac{\partial T_3}{\partial y} = \frac{1}{d}\frac{\partial T_2}{\partial y}, \quad T_2 = T_3, \quad \varphi = 0, \quad \frac{\partial C}{\partial y} - \frac{\partial T_2}{\partial y} = 0; \\ &for \quad y = 1 + \delta, && \frac{\partial T_3}{\partial y} = \frac{-1}{d}. \end{aligned} \quad (5)$$

The full system of equations admits the following equilibrium (i.e. basic) solution: $T_{1,b} = -y/d + T_a, T_{2,b} = T_a - y, T_{3,b} = (1 - y)/d + T_a - 1, \vec{V} = 0, C_b = y - 1/2$,

where T_a is initial non dimensional temperature. Ouattara et al. [19] studied the linear stability of this solution. They found analytically the critical Rayleigh number beyond which this solution loses its stability either via a stationary bifurcation or a Hopf bifurcation.

They showed that, for $\psi \geqslant \psi_{uni}$, with:

$$\psi_{uni} = \frac{51d^2\delta^2 + 70d\delta^3 - 12d\delta - 10}{10Le(1 + 2d\delta)^2 - 51d^2\delta^2 - 70d\delta^3 + 12d\delta + 10}$$

This solution loses its stability via a stationary bifurcation leading to an unicellular flow with the corresponding critical Rayleigh number:

$$Ra_{cs} = \frac{12(1 + 2d\delta)}{1 + \psi(2Led\delta + Le + 1)}.$$

Remark 1: if $d \to \infty$, the walls which delimit the porous layer are infinitely conductive compared to the porous layer saturated by the binary fluid. So, $\psi_{uni} \to 1/((40Le/51) - 1)$ and $Ra_{cs} \to 12/(Le\ \psi)$, a result which has already been obtained by Charrier-Mojtabi et al. [12].

Remark 2: if $\delta \to 0$, the plates become infinitely thin and the heat flux is directly imposed on the porous layer saturated by the binary fluid. So, $\psi_{uni} \to -1/(Le + 1)$ and $Ra_{cs} \to 12/(1 + \psi(Le + 1))$, a result which was found by Yacine et al. [20]. This last result shows that for uniform heat flux imposed on the horizontal walls, it is possible to obtain the separation of the components for any binary solution with positive Soret coefficient, whereas for isothermal boundary conditions this operation is only possible should $\psi \geqslant \psi_{uni} \to 1/((40Le/51) - 1)$ be satisfied [12].

3. Analytical solution of the unicellular flow

3.1. Parallel flow approximation

For the limiting case of a shallow cavity $A >> 1$, we considered the parallel flow approximation which has been used by many authors (c.f. Elhajjar et al. [13]) to determine the velocity (or stream function), the temperature and mass fraction fields. The unicellular flow is then given as follows:

$$\begin{aligned} \varphi_{uni} = \varphi_{uni}(y); \quad T_{1uni} = A_1 x + f_1(y); \quad T_{2uni} = A_2 x + f_2(y); \\ T_{3uni} = A_3 x + f_3(y); \quad C_{uni} = mx + g(y); \end{aligned} \quad (6)$$

where A_i, (i = 1, 2, 3), and m are, respectively, the gradients of the temperatures and mass fraction along the x -axis. With these assumptions and for the steady state, the system given by Eqs. (4) is reduced to a set of ordinary differential equations which may be solved using Maple:

$$\begin{cases} \frac{d^2\varphi_{uni}}{dy^2} = -Ra(A_2 + \psi m), \\ \frac{d^2 f_2}{dy^2} = A_2 \frac{d\varphi_{uni}}{dy}, \\ \left(\frac{d^2 g}{dy^2} - \frac{d^2 f_2}{dy^2}\right) = mLe\frac{d\varphi_{uni}}{dy}, \\ \frac{d^2 f_1}{dy^2} = 0, \\ \frac{d^2 f_3}{dy^2} = 0. \end{cases} \quad (7)$$

Using the boundary conditions (5) and due to the fact that the species are also conserved in time throughout the porous cavity, thereby satisfying $\iint_\Omega C_{uni}(x, y)dxdy = 0$, we obtain the following expression for the stream function:

$$\varphi_{uni} = \psi_0(y - y^2), \text{ with } \psi_0 = \frac{1}{2}Ra(A_2 + \psi m), \tag{8}$$

and the following expressions for $f_1(y), f_2(y), f_3(y)$ and $g(y)$ by integration:

$$\begin{aligned} f_1(y) &= -\frac{y}{d} + \beta; \\ f_2(y) &= -\psi_0 A_2\left(\frac{y^3}{3} - \frac{y^2}{2}\right) - y + \beta; \\ f_3(y) &= -\frac{y}{d} + \frac{\psi_0 A_2}{6} + \frac{1}{d} - 1 + \beta; \\ g(y) &= \frac{\psi_0(A_2 + mLe)(1-2y)(2y^2 - 2y - 1)}{12} + \frac{(1 - mA)}{2} - y; \end{aligned} \tag{9}$$

Expressions for A_2 and m may be found using the fact that, at steady state, the total heat transfer through any cross section perpendicular to the x axis and the mass flow of the component of mass transfer fraction C_{uni} are both zero. We obtain Eqs. (10) and (11):

$$-\int_{-\delta}^{0} \frac{\partial T_{1uni}}{\partial x} dy + \int_0^1 \left(-\frac{\partial T_{2uni}}{\partial x} + T_{2uni}\frac{\partial \varphi_{uni}}{\partial y}\right) dy - \int_1^{1+\delta} \frac{\partial T_{3uni}}{\partial x} dy = 0, \tag{10}$$

and

$$\int_0^1 \left(\frac{\partial \varphi_{uni}}{\partial y} g(y) Le - m + A_2\right) dy = 0, \tag{11}$$

which leads to the following expressions for A_2 and m:

$$A_2 = \frac{5\psi_0}{\psi_0^2 + 30 + 60d\delta}, \text{ and } m = -\frac{Le\psi_0^2 A_2 - 5Le\psi_0 - 30A_2}{Le^2\psi_0^2 + 30}. \tag{12}$$

Due to the continuity of the temperature field inside the cell, we deduce that $A_1 = A_3 = A_2$.

Using the assumptions already mentioned and the corresponding boundary and interface conditions (5), we find the following expressions for the stream function, the mass fraction and the temperature in the three regions:

$$\begin{cases} \varphi_{uni} = \psi_0(1-y)y, \\ T_{1uni} = A_2 x - \frac{y}{d} + \beta, \\ T_{2uni} = A_2 x - \psi_0 A_2(\frac{y^3}{3} - \frac{y^2}{2}) - y + \beta, \\ T_{3uni} = A_2 x - \frac{y}{d} + \frac{\psi_0 A_2}{6} + \frac{1}{d} - 1 + \beta, \\ C_{uni} = mx + \frac{\psi_0(A_2 + mLe)(1-2y)(2y^2 - 2y - 1)}{12} + \frac{(1-mA)}{2} - y. \end{cases} \tag{13}$$

We note that the value, β, is arbitrary due to the Neumann boundary conditions. On combining the expressions for A_2 and m, given in (12), with the expression for ψ_0 it is found that,

$$\psi_0(2Le^2\psi_0^4 - 5d_1\psi_0^2 - 2b^2 d_2) = 0, \tag{14}$$

where,

$$\begin{cases} b = 5/4, \\ d_1 = Ra\ Le^2 - 12[1 + Le^2(1 + 2\delta d)], \\ d_2 = 48Ra[1 + \psi(1 + Le(1 + 2\delta d))] - 5761 + 2d\delta). \end{cases} \tag{15}$$

Eq. (14) admits the trivial solution $\psi_0 = 0$ and the remaining 4th degree equation reduces to a 2nd degree equation.

From the above result, it follows that the solutions of Eq. (14) are:

$$\psi_0 = \left[0, \pm\frac{\sqrt{b}}{Le}\left(d_1 \pm \sqrt{d_1^2 + Le^2 d_2}\right)^{1/2}\right]. \tag{16}$$

Eq. (16) indicates that five solutions are possible. One of these solutions, namely $\psi_0 = 0$, corresponds to the rest state, and while this is always possible it may not stable. The first signs + and – correspond to counterclockwise and clockwise unicellular circulations respectively. Due of the property of symmetry, specific to the horizontal configuration, the unicellular flows are symmetrical in pairs. This result is obtained with Eq. (16) giving the values of $\pm\psi_0$. The direction of rotation of the convective cells is defined by the stream function $\psi_0(1-y)y$ (Eq. (12)). Moreover, the sign of the mass gradient m is directly connected to ψ_0 (Eq. (18)). For laboratory experiments, to induce a flow in one direction or the other, it is sufficient to tilt the cell, very slightly compared to the horizontal and return to the horizontal situation once the unicellular flow is established.

As indicated by the relation (16), if: $d_1^2 + Le^2 d_2 < 0$, the Eq. (14) has 4 imaginary roots. Then, only the equilibrium solution is possible. If $d_2 > 0 \Rightarrow d_1^2 + Le^2 d_2 > 0$, in addition the product of the roots of this 2nd degree equation in ψ_0^2 is positive then the Eq. (14) has, in addition to the equilibrium solution, two real and two imaginary solutions; $d_2 > 0 \Rightarrow$ Ra $(1 + \psi(2Led\delta + Le + 1)) > 12(1 + 2d\delta)$ and this inequality leads to:

$$\begin{cases} \psi > -\frac{1}{1+Le(1+2d\delta)} \Rightarrow Ra > Ra_{cs} = \frac{12(1+2d\delta)}{1+\psi(1+Le+2Led\delta)} \\ \psi < -\frac{1}{1+Le(1+2d\delta)} \Rightarrow Ra > Ra_{cs} = \frac{12(1+2d\delta)}{1+\psi(1+Le+2Led\delta)} \end{cases}. \tag{17}$$

Using the analytical solution of the unicellular flow, we determined indirectly the critical Rayleigh number beyond which the equilibrium solution loses its stability [14].

On studying the sign of the discriminant of this 2nd degree algebraic equation, we determined that there are three regions (I, II, III) in $(\psi,\ Ra)$ space where this equation admits, respectively, 0, 2, or 4 real solutions associated with different flow structures. In Fig. 2 we present, for $Le = 3$, $d = 1$, $\delta = 0.01$, these different regions of (Ra, ψ) -space and the various analytical expressions of different curves delimiting the three regions of the plane $(\psi,\ Ra)$.

3.2. Optimization of the dimensional separation gradient

The separation, $S = mA$, is defined as the difference in the mass fractions of the denser component in the vicinity of left and right vertical walls of the horizontal cell.

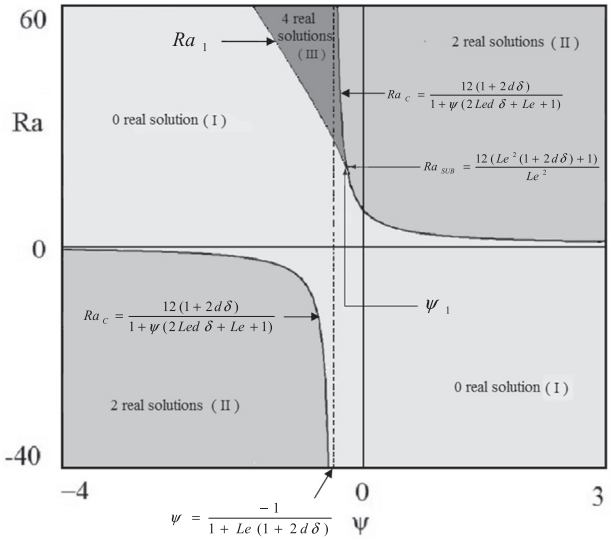

Fig. 2. Various analytical expressions of different curves delimiting the regions of the plane $(\psi,\ Ra)$ where the problem admits 0, 2 or 4 real solutions. $(Le = 3,\ d = 1,\ \delta = 0.01)$. $\psi_1 = \dfrac{-1}{2d\delta Le[1 + Le + 2Le^2(1 + d\delta)] + 1 + Le + Le^2 + Le^3}$ and $Ra_1 = \dfrac{12(Le - 2\psi)(1 + 2d\delta) + 1) - (Le + 1) + 2\left[-\psi(2Led\delta + Le + 1)(2Led\delta(Le^2 - \psi) + (Le + 1)(Le - \psi - 1)\right]^{1/2}}{Le^2}$.

On replacing A_2 by its value in the expression for m (Eq. (12)), we obtain an expression for m as a function of ψ_0. The dimensionless mass fraction is then given by:

$$m = \frac{150\psi_0(2Led\delta + Le + 1)}{(Le^2\psi_0^2 + 30)(60d\delta + \psi_0^2 + 30)}, \tag{18}$$

where ψ_0 is a non-zero root of the Eq. (14). Eq. (14) may be solved easily for Ra:

$$Ra = \frac{2(Le^2\psi_0^2 + 30)(60d\delta + \psi_0^2 + 30)}{5(Le^2\psi_0^2 + 60Led\delta\psi + 30Le\psi + 30\psi + 30)}, \tag{19}$$

where $Ra = (g\beta_T K\Delta TH)/(a\nu) = F\Delta TH$ with $F = (g\beta_T K)/(a\nu)$.

The dimensional value of the separation between the ends of the cavity is given by: $S^r = m^r L = C_0(1-C_0)\frac{D_T}{D}\Delta TmL/H$ where: $m^r = C_0(1-C_0)\frac{D_T}{D}\frac{\Delta T}{H}m = E\frac{\Delta T}{H}m$ with $E = C_0(1-C_0)\frac{D_T}{D}$. The non-dimensional mass fraction m is only function of $Ra = F\delta TH$ whereas the expression m^r is doubly dependent on ΔT: $m^r = E\frac{\Delta T}{H}m(F\Delta TH)$.

For a given binary solution in a cavity of length L, the optimal separation corresponds to the maximum of m^r as a function of the two variables H and ΔT. This optimum exists if the following system of equations admits a solution

$$\begin{cases} \frac{\partial m^r}{\partial H} = \frac{E\Delta T}{H}\left(-\frac{m}{H} - F\Delta T\frac{dm}{dRa}\right) = 0 \Rightarrow m = Ra\frac{dm}{dRa} \\ \frac{\partial m^r}{\partial \Delta T} = \frac{E}{H}\left(m + F\Delta TH\frac{dm}{dRa}\right) = 0 \quad \Rightarrow m = -Ra\frac{dm}{dRa} \end{cases} \tag{20}$$

The system (20) admits only a single solution, $m = 0$. Hence this problem admits an optimum which is only function of H for fixed ΔT or as a function of ΔT for fixed H (cf. Fig. 3 given m^r, which is function of H and δT). We observe that the mass fraction m^r varies weakly when ΔT increases for fixed H. For fixed values of H, the equation $m + Ra\frac{dm}{dRa} = 0$ leads to $m\frac{dRa}{d\psi_0} + Ra\frac{dm}{d\psi_0} = 0$.

This last equation depends only on ψ_0 since Ra, m, $\frac{dRa}{d\psi_0}$, $\frac{dm}{d\psi_0}$ are functions solely of the following fourth degree equation for ψ_0:

$$Le^2\psi_0^4 + (20Le^2d\delta + 10Le^2 + 10)\psi_0^2 - 600d\delta - 300 = 0 \tag{21}$$

Once the roots, ψ_{0P}, of this algebraic equation have been found, the value of the optimal Rayleigh number Ra_{op}, is obtained by replacing ψ_{0P} by its expression in Eq. (19). $Ra_{op} = F\Delta T_{op}H$ is thus fixed, which implies that ΔT_{op} is also fixed since F and H are fixed. The maximum value for m^r is then given by:

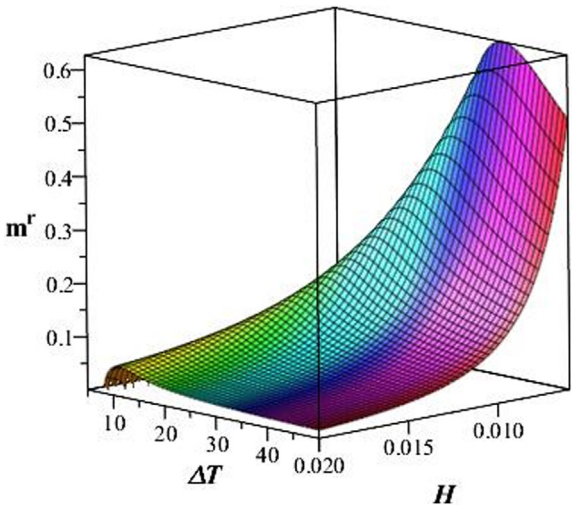

Fig. 3. Real mass fraction gradient m^r, function of the temperature difference ΔT and the cell thickness H, for Le = 5, $\psi = 0.1$, $\delta = 0$, d = 4.

$$m^r = E\frac{\Delta T_{op}}{H}m(F\Delta T_{op}H) \tag{22}$$

The analytical expressions of ψ_{0P}, Ra_{op} and ΔT_{op} are determined with Maple software, but are too lengthy to include here. In order to illustrate the results, we only give their associated numerical expressions for fixed values of Le, ψ, δ and d:

For Le = 100, ψ = 0.1, d = 29 and δ = 1, 0, we obtain respectively ψ_{0P} = 0.0548, 0.0547, Ra_{op} = 2.391, 1.983 and ΔT_{op} = 21.055, 17.462. We therefore deduce that:

$$\frac{m^r_{\max}(\delta = 1)}{m^r_{\max}(\delta \to 0)} = \frac{0.4569}{0.4609} = 0.991.$$

For Le = 232, ψ = 0.1, d = 29 and δ = 1, 0, we obtain respectively ψ_{0P} = 0.0236, 0.0236, Ra_{op} = 1.033, 0.949 and ΔT_{op} = 9.097, 8.353. We therefore deduce that:

$$\frac{m^r_{\max}(\delta = 1)}{m^r_{\max}(\delta \to 0)} = \frac{0.4566}{0.4584} = 0.996.$$

For Le = 232, ψ = 0.2, d = 29 and δ = 1, 0, we obtain respectively ψ_{0P} = 0.0236, 0.0236, Ra_{op} = 0.517, 0.494 and ΔT_{op} = 4.553, 4.350. We therefore deduce that:

$$\frac{m^r_{\max}(\delta = 1)}{m^r_{\max}(\delta \to 0)} = \frac{0.4566}{0.4584} = 0.996.$$

We note that the change from ψ = 0.1 to ψ = 0.2, which corresponds to many binary mixtures with a positive Soret coefficient, slightly modifies the optimal parameters defined previously. For larger values of the Rayleigh number, Ra = 10, Le = 232, ψ = 0.2, d = 29 and δ = 1, 0, we obtain respectively ψ_0 = 0.146, 0.355 and m = 0.144, 0.060. We thus deduce theoretically and numerically, for a cavity with an aspect ratio equal to 10 the separation values, S = 1.44, 0.60, as indicated in Fig. 6. We can conclude that the optimum separation is not modified by taking into account the characteristics of the walls. By contrast, the value of S is strongly affected for large values of Ra. The measurements of the mass fraction gradient are made for temperature differences very much higher than those leading to the optimum of separation. The calculation of the thermodiffusion coefficients from these measurements would therefore be imprecise if we do not take into account the nature and the thickness of the walls.

4. Numerical simulations

This problem has also been studied numerically by solving system (4) with the associated boundary (5) using a finite element method (as provided by the COMSOL Multiphysics software). We considered two bounded domains with A = 10 and A = 20, since we wish to compare the results for this confined geometry to those obtained analytically for a cell of large aspect ratio, $A >> 1$. We used a rectangular grid system, which is better-suited to the rectangular shape of the cavity. The spatial resolution was: 200 × 30 for A = 10 and 300 × 50 for A = 20. We will show that the numerical results are quite the same for the central portion of the cavity for the two cases, which shows that the parallel flow approximation used earlier is accurate.

It was stated earlier that the separation is defined as the difference of the mass fraction of the denser species between the two ends of the cavity: $S = mA$. In order to reduce the perturbation effects on the calculation of S due to the nonparallel flow near the two vertical sidewalls, we plot the curve $C = f(x)$ at a given value of y (y = 0.5, for instance) and we calculate the slope of the curve, which is a straight line except near the vertical sidewalls of the cavity. The values of the slope obtained analytically are found to be in good agreement with the numerical results.

To illustrate our study, we consider the water/ethanol mixture used by Platten et al. [21], with water (60.88 wt%) and $\psi = 0.2$. The average temperature of the mixture was 22.5 °C. The properties of this binary mixture for $T = 22.5$ °C are given in Table 2. The studied cell was made of copper alloy with 1 cm thick horizontal plates, 1 cm thick porous layer and its length was 10 cm. The cavity was filled with a porous medium consisting of glass spheres saturated by the water/ethanol mixture.

Due to thermodiffusion, and for $\psi > 0$, the denser component of the mixture moves towards the cold wall at the top of the cell and the other one moves towards the hot wall at the bottom of the cell. This unicellular flow advects one of the components of the mixture towards the right hand end of the cavity and the other one towards the left hand end, and this leads to a horizontal stratification of the concentration field. Figs. 4 and 5 show the *iso*-concentrations and the streamlines for $Le = 232$, $\psi = 0.2$, and $Ra = 4$ with and without the influence of walls ($d = 29$, $\delta = 1$) and ($d = 0$, $\delta = 0$), and we obtain $S = 2.04$ and $S = 1.86$, respectively. It is essential to note that the importance of species separation is underestimated by not taking into account the influence of the surface thicknesses.

Fig. 6 shows the variation of separation with the Rayleigh number, Ra, for $Le = 232$ and $\psi = 0.2$ with ($d = 29$ and $\delta = 1$).

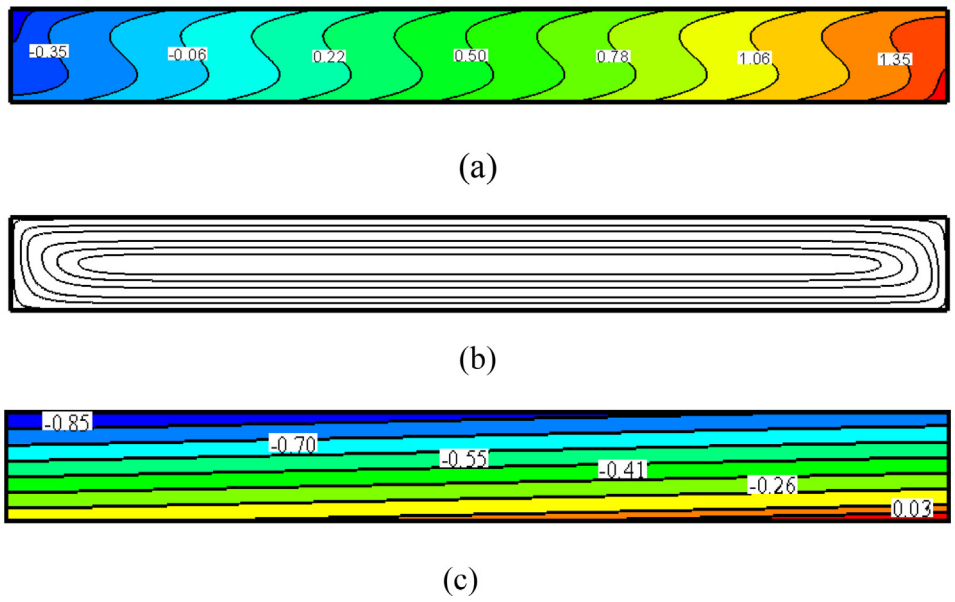

Fig. 4. Isoconcentrations (a) and streamlines (b) and isotherms (c) for Le = 232, $\psi = 0.2$, $Ra = 4$, (without taking account the presence of the walls), $S = 1.86$.

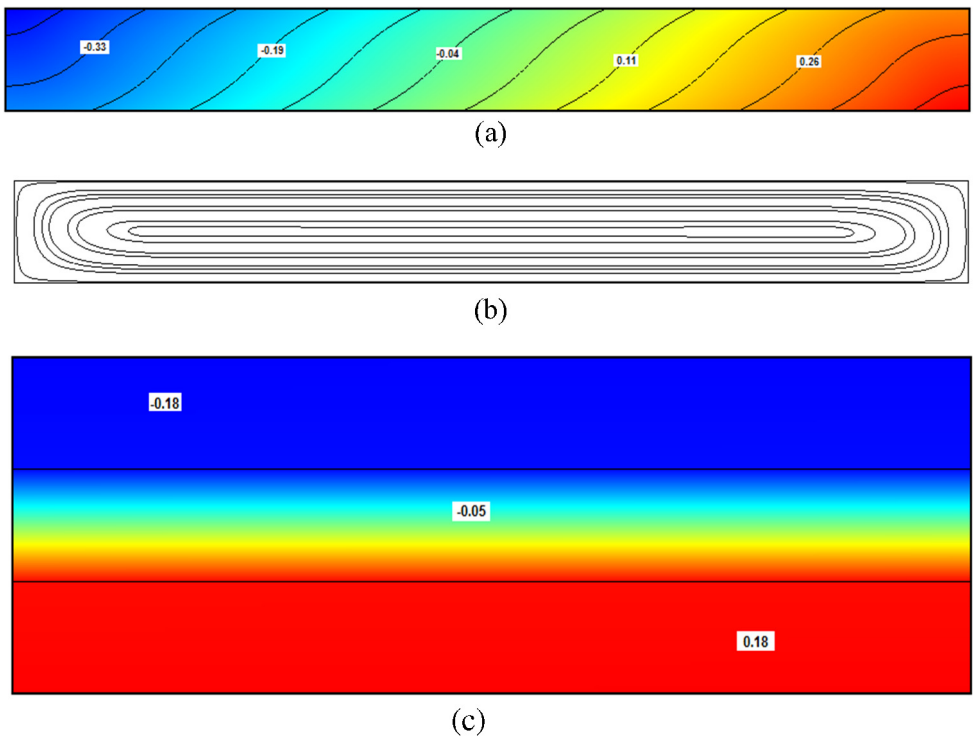

Fig. 5. Isoconcentrations (a), streamlines (b) and isotherms (c) for Le = 232, $\psi = 0.2$, Ra = 4, $d = 29$, δ=1, $S = 2.04$.

and without ($d = 0$, $\delta = 0$) the influence of the walls. It should be noted that, due to the reference scale used for the concentration field, the separation S may be greater than 1. The optimum separation has the same value with or without influence of the walls but it varies significantly when $Ra \geqslant 2.5$. These numerical results are in good agreement with the theoretical part developed in Section 3.2. The analytical solution predicted by the present theory, as represented by the solid line, is observed to be in very good agreement with the numerical results represented by the black dots.

5. Linear stability analysis of the unicellular flow

In order to study the stability of the unicellular solution $(\varphi_{uni}, T_{1uni}, T_{2uni}, T_{3uni}, C_{uni})$, it is convenient to rewrite the governing equations using the perturbations of the stream function ϕ, temperature $\theta_1, \theta_2, \theta_3$ and concentration c:

$$\phi = \tilde{\varphi}_{uni} - \varphi_{uni}; \quad \theta_1 = \tilde{T}_{1uni} - T_{1uni}; \quad \theta_2 = \tilde{T}_{2uni} - T_{2uni};$$
$$\theta_3 = \tilde{T}_{3uni} - T_{3uni}; \quad c = \tilde{C}_{uni} - C_{uni}; \tag{23}$$

where $(\tilde{\varphi}_{uni}, \tilde{T}_{1uni}, \tilde{T}_{2uni}, \tilde{T}_{3uni}, \tilde{C}_{uni})$ are the disturbance fields. The disturbances are developed in normal modes as the cell is quite of infinite extension:

$$(\varphi, \theta_1, \theta_2, \theta_3, c) = [\varphi(y), \theta_1(y), \theta_2(y), \theta_3(y), c(y)] \exp(ikx + \sigma t) + c.c,$$

In the above expansion, the disturbances $(\varphi(y), \theta_1(y), \theta_2(y), \theta_3(y), c(y))$ are the amplitudes of the stream function, temperatures and the mass fraction, the value k is the wave number in the horizontal direction and σ is the temporal exponential growth rate of the perturbations. We introduce the new variable, $\eta = c - \theta_2$, for convenience. The system of linear ordinary differential equations can be written as:

$$\begin{cases} (D^2 - k^2)\phi = -iRak[\theta_2(1+\psi) + \psi\eta], \\ (D^2 - k^2)\theta_2 = \sigma\theta_2 + ik\theta_2 \frac{\partial \phi_{uni}}{\partial y} + A_2 \frac{\partial \phi}{\partial y} - ik\phi \frac{\partial T_{2uni}}{\partial y}, \\ (D^2 - k^2)\eta = Le\left(\varepsilon\sigma + ik\frac{\partial \phi_{uni}}{\partial y}\right)(\eta + \theta_2) + mLe\frac{\partial \phi}{\partial y} - ik\varphi Le\frac{\partial C_{uni}}{\partial y}, \\ (D^2 - k^2)\theta_1 = \frac{\sigma\theta_1}{\alpha}, \\ (D^2 - k^2)\theta_3 = \frac{\sigma\theta_3}{\alpha}. \end{cases} \tag{24}$$

where $D = \partial/\partial y$. The corresponding boundary conditions are:

$$\begin{aligned} &\text{for } y = -\delta, && \frac{\partial \theta_1}{\partial y} = 0; \\ &\text{for } y = 0, && \frac{\partial \theta_1}{\partial y} = \frac{1}{d}\frac{\partial \theta_2}{\partial y}, \quad \theta_1 = \theta_2, \quad \phi = 0, \frac{\partial \eta}{\partial y} = 0; \\ &\text{for } y = 1, && \frac{\partial \theta_3}{\partial y} = \frac{1}{d}\frac{\partial \theta_2}{\partial y}, \quad \theta_2 = \theta_3, \quad \phi = 0, \frac{\partial \eta}{\partial y} = 0; \\ &\text{for } y = 1 + \delta, && \frac{\partial \theta_3}{\partial y} = 0. \end{aligned} \tag{25}$$

The results of direct numerical simulations show that the unicellular solution loses its stability via a stationary bifurcation.

For Le = 232, d = 29, δ = 1 and $\psi = 0.1 > \psi_{uni} = 0.022$, we deduce the value of the critical Rayleigh number leading to the onset of the unicellular flow: $Ra_{c0} = 0.52$. Starting from this first transition, we found only the unicellular flow for Ra slightly higher than Ra_{c0}. Gradually increasing the Rayleigh number value, we found not only unicellular flow but another bi-cellular flow also stable. This bi-cellular flow was obtained only by modifying the initial conditions. Continuing this procedure, we found not only these two types of solutions but a flow with three convective cells and then the unicellular flow and flows with 2, 3, 4 cells equally stable, again with $Ra < Ra_{c1} = 46$. When the unicellular flow loses its stability, for $Ra > 46 = Ra_{c1}$, the other flows maintain their stability up to values higher than Ra_{c1}. Multiple variety of multicellular flows (with two to eleven cell structure) exist and are linearly stable even for $Ra < 46$ and for a large range of values of $Ra > Ra_{c1}$. This peculiarity for a horizontal porous layer saturated by binary mixture and subjected to vertical uniform heat flux differs from the classical case where the horizontal cell is heated from below and where the horizontal walls are maintained at **uniform** constant temperatures T_1 and T_2.

The maximum value of the stream function and the kinetic energy as a function of the Rayleigh number, for unicellular flow, *are represented* respectively in Figs. 7 and 8 for *Le = 232,d = 29, δ = 1.* The analytical solution obtained is in good agreement with the results of direct numerical simulation.

We restrict ourselves in this study to this stationary transition for positive separation ratios. In this case, the mechanical equilibrium solution loses its stability via stationary bifurcation and leads to a unicellular flow only for values of $\psi \geqslant \psi_{uni}$.

The resulting linear problem is solved by means of a sixth order pseudo Tau-Galerkin method. The boundary conditions for $\varphi(y)$ and $\eta(y)$ are known so the following expansions, which satisfy these boundary conditions, are used:

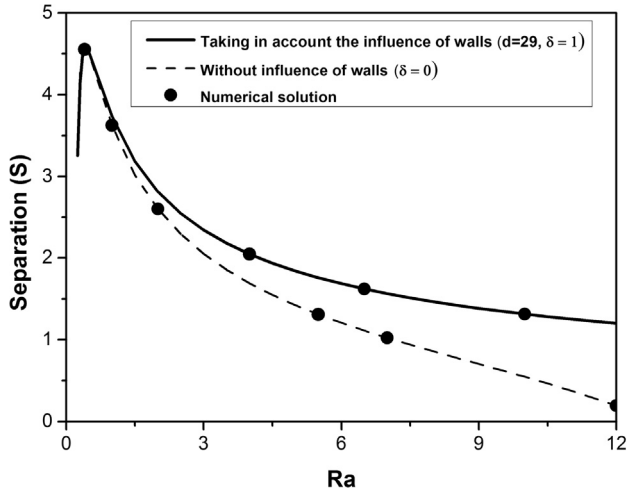

Fig. 6. Separation versus Rayleigh number for Le = 232, $\psi = 0.2$, d = (0, 29) and δ = (0, 1).

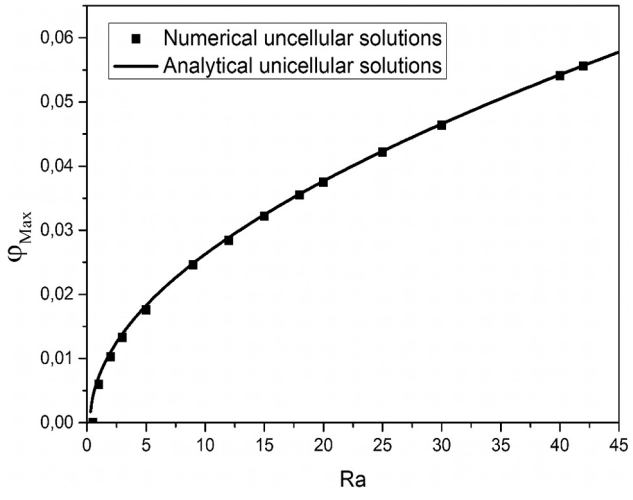

Fig. 7. Maximum stream function versus Rayleigh number for unicellular solution. For Le = 232, $\psi = 0.2$, d = 29 and δ = 1.

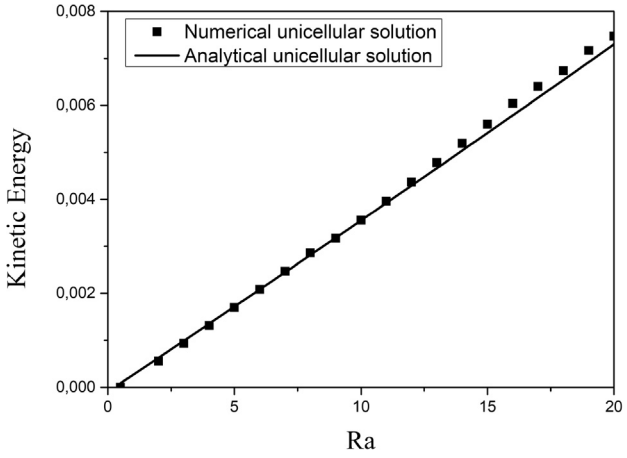

Fig. 8. Kinetic energy versus Rayleigh number for unicellular solution. For Le = 232, $\psi = 0.2$, $d = 29$ and $\delta = 1$.

$$\varphi(y) = \sum_{n=1}^{N} f_n (1-y) y^n \quad and$$

$$\eta(y) = d_1 + d_2\left(y^2 - \frac{2}{3}y^3\right) + \sum_{n=1}^{N-2} d_{n+2} y^{n+1}(1-y)^2.$$

Using the boundary conditions: $\frac{\partial \theta_1(y=-\delta)}{\partial y} = 0$ *and* $\frac{\partial \theta_3(y=1+\delta)}{\partial y} = 0$ the general solutions of the perturbation equations for the bounding plates are given respectively by:

$$\theta_1(y) = B_1(e^{k(y+2\delta)} + e^{-ky}) \text{ and } \theta_3(y) = B_3(e^{k(y-2(1+\delta))} + e^{-ky}).$$

The four boundary conditions, (25), which are associated with the perturbation $\theta_2(y)$, are all coupled to the perturbations $\theta_1(y)$ and $\theta_3(y)$. The function $\theta_2(y)$ is then written in the following polynomial form: $\theta_2(y) = \sum_{i=1}^{i=N} b_i y^{i-1}$.

The writing of these four boundary conditions satisfied by $\theta_2(y)$ allows the determination of the first four coefficients ($b_i, i = 1$ *to* 4) of $\theta_2(y)$ function of B_1 and B_3 and b_i for $i > 4$.

The critical values of the Rayleigh number Ra_{co2} and wave number k_{co2}, are obtained for $\psi = 0$ and for four values of $\psi \geqslant \psi_{uni}$ using approximations from the third to the sixth order.

Table 1
Critical values of Rayleigh number Ra_{c2} and the wave number k_{c2} associated with the transition from the unicellular to multicellular one, Le = 232, $d = 29$, $\delta = 3$, $\varepsilon = 0.5$ and for different values of $\psi \geqslant \psi_{uni}$ and three order approximations.

Le = 232, d = 29, δ=3	4th order		5th order		6th order	
ψ	k_{c2}	Ra_{c2}	k_{c2}	Ra_{c2}	k_{c2}	Ra_{c2}
0	3.22	43.06	3.08	38.58	3.08	38.56
0.1	3.31	46.54	3.24	46.81	3.24	46.91
0.4	3.28	47.85	3.24	46.91	3.24	47.28
0.5	3.27	48.53	3.24	47.25	3.24	47.28
0.6	3.26	49.23	3.24	47.62	3.24	47.29

The Lewis number, Le, the thermal conductivity ratio, d and the aspect ratio, δ are set at $(Le, d, \delta) = (232, 29, 3)$. The case, $Le = 232$ corresponds to a liquid binary mixture, like water/ethanol or water/isopropanol with appropriate mass fraction. We recall that we have already found that the flow is unicellular when $\psi \geqslant \psi_{uni} = 0.00623$. When $\psi = 0.1$, the linear stability analysis of the equilibrium solution leads respectively to: $Ra_{c1} = 0.517$. This unicellular flow loses its stability at $Ra_{c2} = 46.91$ and $k_{c2} = 3.24$ at sixth order. These results are illustrated in Table 1. It should be noted that the critical Rayleigh number increases and the critical wave number decreases when the separation ratio increases. The results which were obtained for pure fluid ($\psi = 0$) are in good agreement with those found in [17].

6. Conclusion

In this paper, an analytical and numerical analysis of the species separation of a binary mixture saturating a porous layer was presented, taking into account the influence of the bounding plates of the cell. The cavity is bounded above and below by two thin horizontal and impermeable plates of uniform thickness. These plates are subjected to a uniform heat flux.

The equations were nondimensionalised in such a way that the filtration Rayleigh number is based on magnitude of the applied heat flux applied on the upper and lower sublayers. In addition to the classical dimensionless parameters of the problem without the bounding plates being present, two further parameters are required, namely the conductivity ratio between the solid and porous sublayers, d, and the relative thickness of the bounding plates, δ.

The main objective of this study concerned the influence of the thickness and the nature of the bounding plates on the thermogravitational separation of the constituents of a binary mixture saturating a porous medium. This separation is possible only in the presence of a unicellular flow. This unicellular flow should also be linearly stable. Numerical simulations and the linear stability of the unicellular flow were then performed. It appears that for binary solutions with $\psi \geqslant \psi_{uni}$, and for example (Le = 232, ψ = 0.2, $d = 29$, $\delta = 3$), the mechanical equilibrium solution gives rise to a unicellular flow for $Ra_{c1} = 0.26$ and the unicellular flow gives rise to a multicellular flow for $Ra_{c2} = 47$ and $k_{c2} = 3.24$. The species separation is therefore possible for a wide range of Rayleigh numbers [0.26, 47]. Moreover the optimal separation is obtained for a $Ra_{op} = 0.52 \in [0.26, 47]$, a domain within which the unicellular flow is linearly stable.

Knowing the characteristics (Le, ψ) of the binary mixture saturating a porous cavity defined by d and δ, the theoretical study allowed us to obtain the Ra_{op} et m^{Γ}_{op} values leading to the optimal species separation. All the results obtained analytically have been validated numerically. Moreover, we validated our results by comparing them with the results obtained in three limiting cases: infinitely thin walls ($\delta \to 0$), infinitely conducting walls ($d \to \infty$) and a mono-constituent fluid ($\psi \to 0$).

We have shown that the optimal value of the species separation of the binary mixture does not depend on the thickness or the

Table 2
Properties for a water (60.88 wt%) - ethanol (39.12 wt%) mixture at a mean temperature of 22.5 °C.

β_T	β_C	ρ	D	D_T	λ_f	υ	a
$7.86 \cdot 10^{-4}$ K^{-1}	−0.212 –	935.17 $kg{\cdot}m^{-1}$	$4.32 \cdot 10^{-10}$ $m^2\ s^{-1}$	$1.37 \cdot 10^{-12}$ $m^2\ s^{-1}\ K^{-1}$	0.267 $W{\cdot}m^{-1}{\cdot}K^{-1}$	$2.716 \cdot 10^{-6}$ $m^2\ s^{-1}$	10^{-7} $m^2{\cdot}s^{-1}$
a^*			D^*				D_T^*
$2.63 \cdot 10^{-7}$ $m^2{\cdot}s^{-1}$			$1.89 \cdot 10^{-10}$ $m^2\ s^{-1}$				$6.01 \cdot 10^{-12}$ $m^2\ s^{-1}\ K^{-1}$

nature of the walls. On the other hand, this optimal separation is obtained for very small values of the Rayleigh number (which also corresponds to very small porous layer thickness). Experiments leading to significant species separation to measure thermodiffusion coefficients are performed for larger values of Ra. In this case, species separation strongly depends on the characteristics of the walls.

Acknowledgments

This research was supported by the CNES (Centre National d'Études Spatiales) Toulouse, France.

References

[1] D.A. Nield, A. Bejan, Convection in Porous Media, third ed., Springer, New York, 2006.
[2] D.B. Ingham, I. Pop, Transport Phenomena in Porous Media, vol. III, Elsevier Sciences, Amsterdam, 2005
[3] Vafai, Handbook of Porous Media, second ed., Taylor & Francis, New York, 2005, pp. 269–320.
[4] P. Vadász, in: Peter Vadász (Ed.), Theory and Applications of Transport in Porous Media, vol. 22, Springer, 2008, Hardcover ISBN: 978-1-4020-8177-4.
[5] A. Zebib, M.M. Bou-Ali, Inclined layer Soret instabilities, Phys. Rev. E 79 (2009) 056305.
[6] K. Clusius, G. Dickel, Neues Verfahrenzur Gasenmisschung und isotropennung, Naturwisse 26 (1938) 546.
[7] W.H. Furry, R.C. Jones, L. Onsager, On the theory of isotope separation by thermal diffusion, Phys. Rev. 55 (1939) 1083–1095.
[8] M. Lorenz, A.H. Emery, The packed thermal diffusion column, Chem. Eng. Sci. 11 (1) (1959) 16–23.
[9] R. Bennacer, A.A. Mohamad, M. El Ganaoui, Thermodiffusion in porous media, Multi-domain constituent separation, Int. J. Heat Mass Transfer 52 (2009) 1725–1733.
[10] M. Marcoux, M.C. Charrier-Mojtabi, M. Azaiez, Double diffusive convection in an annular vertical porous layer, Int. J. Heat Mass Transfer 42 (1999) 2313–2325.
[11] O. Abahri, D. Sadaoui, K. Mansouri, A. Mojtabi, M.C. Charrier-Mojtabi, Thermogravitational separation in horizontal annular porous, Mech. Industry 18 (1) (2017) 106.
[12] M.C. Charrier-Mojtabi, B. Elhajjar, A. Mojtabi, Analytical and numerical stability analysis of Soret-driven convection in a horizontal porous layer, Phys. Fluids 19 (12) (2007) 124104.
[13] B. Elhajjar, M.C. Charrier-Mojtabi, A. Mojtabi, Separation of a binary fluid mixture in a porous horizontal cavity, Phys. Rev. E 77 (2) (2008) 026310.
[14] M.C. Charrier-Mojtabi, B. Elhajjar, B. Ouattara, A. Mojtabi, P. Costesèque, Soret-driven convection and separation of binary mixtures in a porous horizontal slot submitted to a heat flux, C. R. Mécanique 339 (2011) 303–309.
[15] F. Croccolo, F. Scheffold, A. Vailati, Effect of a marginal inclination on pattern formation in a binary liquid mixture under thermal stress, Phys. Rev. Lett. 111 (2013) 014502.
[16] D.N. Riahi, Nonlinear convection in a porous layer with finite conducting boundaries, J. Fluid Mech. 129 (1983) 153–171.
[17] A. Mojtabi, D.A.S. Rees, The effect of conducting bounding plates on the onset of Horton-Rogers-Lapwood convection, Int. J. Heat Mass Transfer 54 (2010) 293–301.
[18] D.A.S. Rees, A. Mojtabi, The effect of conducting boundaries on weakly nonlinear Darcy-Bénard convection, Trans. Porous Med. 88 (1) (2016) 45–63.
[19] B. Ouattara, A. Khouzam, A. Mojtabi, M.C. Charrier-Mojtabi, Analytical and numerical stability analysis of Soret-driven convection in a horizontal porous layer: the effect of conducting bounding plates, Fluid Dyn. Res. 44 (3) (2012) 031415.
[20] L. Yacine, A. Mojtabi, R. Bennacer, A. Khouzam, Soret-driven convection and separation of binary mixtures in a horizontal porous cavity submitted to cross heat fluxes, Int. J. Therm. Sci. 104 (2016) 29–38.
[21] J.K. Platten, M.M. Bou-Ali, J.F. Dutrieux, Enhanced molecular separation in inclined thermogravitational columns, J. Phys. Chem. B 107 (42) (2003) 11763–11767.